Tectonic evolution of the Circum-Moesian orocline of the Carpatho-Balkanides: Paleomagnetic constraints

Emő Márton, Vesna Cvetkov, Miodrag Banješević, Gábor Imre, Aleksandar Pačevski

Journal of Geodynamics 162 (2024) 102058

Contents lists available at ScienceDirect

Journal of Geodynamics

journal homepage: www.elsevier.com/locate/jog

Tectonic evolution of the Circum-Moesian orocline of the Carpatho-Balkanides: Paleomagnetic constraints

Emő Márton [a,*], Vesna Cvetkov [b], Miodrag Banješević [c], Gábor Imre [a], Aleksandar Pačevski [b]

[a] SARA Geological Survey, Paleomagnetic Laboratory, Columbus 17-23, Budapest 1145, Hungary
[b] University of Belgrade, Faculty of Mining and Geology, Đušina 7, Belgrade 11000, Serbia
[c] University of Belgrade, Technical Faculty in Bor, Bor, Serbia

ARTICLE INFO

Keywords:
Apuseni-Banat-Timok-Srednogorie belt
Danubicum
Paleomagnetism
Oroclinal bending

ABSTRACT

The areas of the present study in eastern Serbia, the Danubicum and the Timok Magmatic Complex (TMC, part of the Geticum) are situated between the Vardar Zone and Moesia. The first is Moesia derived and thrust over the Geticum during the latest Cretaceous, the second represents the central segment of the subduction related Apuseni-Banat-Timok-Srednogorie (ABTS) metallogenic belt. The new results, based on 18 geographically distributed sampling points (228 field oriented drill cores) imply large CW vertical axis rotations for the Upper Jurassic (Lower Cretaceous) carbonates of the Danubicum and a moderate one for the Upper Cretaceous igneous and sedimentary rocks from the TMC. These, together with earlier published paleomagnetic data provide kinematic constraints to test the circum-Moesian backarc-convex orocline model. The strike test plot clearly documents that it is a progressive arc. The starting situation at the time of the volcanic activity in the metallic belt (90–70 Ma) must have been a generally E-W oriented S segment, continuing in NNW-SSE oriented ABT segments. The present geometry of the circum-Moesian belt, in the context of Miocene paleomagnetic results from the Vardar Zone and the Apuseni Mts, is interpreted as the result of two main tectonic processes. The first is an about 30° vertical axis CW rotation which took place in coordination with the Vardar Zone (20–17 Ma). The second is an additional 40–65° CW rotation (17–15 Ma) involving also the Danubicum, due to the subduction pull of the E Carpathians in combination with the corner effect of Moesia.

1. Introduction

The present study encompasses the Danubian imbricated area (Danubicum) and the Timok Magmatic Complex. Both are situated between the Vardar zone and Moesia, east of the Serbo-Macedonian composite terrain and belong to the arcuated loop of the backarc-convex orocline related to Moesia (Fig. 1a and b). The formation of the loop is attributed to coeval rotations and docking against Moesia during the Cretaceous–Miocene closure of the Alpine Tethys ocean (e.g. Csontos and Vörös, 2004, Maţenco, 2017) and to the Late Oligocene – Middle Miocene formation of one of the largest strike-slip systems of continental Europe, which accumulated more than 100 km of dextral offset along the curved Cerna and Timok Fault systems (Berza and Draganescu, 1988; Ratschbacher et al., 1993; Kräutner and Krstić, 2002, 2003).

The two areas of the present study, however, have different pre-closure history. The Timok Magmatic Complex belongs to the Getic units (Fig. 1b), which is regarded as the product of the shortening of the Dacia megaunit (Kräutner and Krstić, 2002). Both, the Getic s.s. and the Supragetic units are thick-skinned nappe stacks affected by extension in the Late Cretaceous and also magmatism in the Apuseni-Banat-Timok-Srednogorie belt (ABTS, Berza et al., 1998; von Quadt et al., 2005). The ABTS is part of the transcontinental Tethyan-Eurasian Metallogenic Belt (Janković, 1977), in which the Timok Magmatic Complex almost totally overlap with the economically very important Bor Metallogenetic Zone (BMZ). The BMZ hosts more than hundred significant Cu-Au and polymetallic mineralizations, out of which 22 have been recorded as ore deposits (see review of Jelenković et al., 2016). Five world-class copper deposits are presently in operation: Majdanpek, Veliki Krivelj, the large Bor hydrothermal system, Cerovo and the recently discovered Čukaru Peki copper and gold hydrothermal system.

* Corresponding author.
E-mail addresses: paleo@mbfsz.gov.hu (E. Márton), vesna.cvetkov@rgf.bg.ac.rs (V. Cvetkov), mbanjesevic@tfbor.bg.ac.rs (M. Banješević), aleksandar.pacevski@rgf.bg.ac.rs (A. Pačevski).

https://doi.org/10.1016/j.jog.2024.102058
Received 20 March 2024; Received in revised form 23 August 2024; Accepted 12 September 2024
Available online 12 September 2024

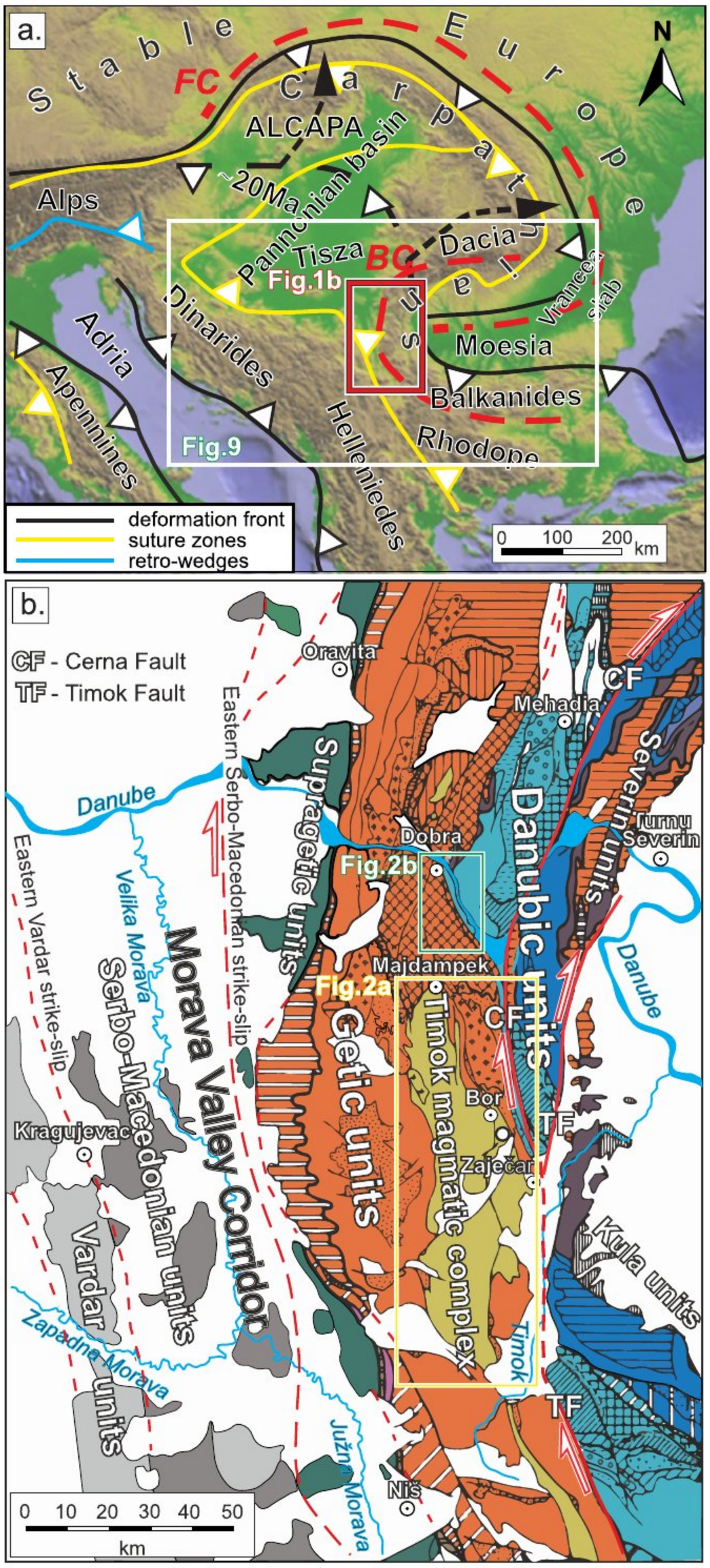

Fig. 1. Simplified image of the Mediterranean orogen (Fig. 1a) deformed during Mesozoic and Cenozoic times (modified after Krstekanić et al., 2020) outlining foreland-convex (FC) and back-arc convex (BC) oroclines. Red rectangle shows the location of the tectonic map of Fig. 1b (modified after Kräutner and Krstić, 2003) and the white rectangle shows the location of Fig. 9.

The geology of the ABTS, due to its economic importance, has been intensively studied during the last decades (e.g. von Quadt et al., 2002; Clark and Ullrich, 2004; Lips et al., 2004; von Quadt et al., 2005; Zimmerman et al., 2008; Kolb et al., 2013; Gallhofer et al., 2015; Knaak et al., 2016, Banješević et al., 2019). Some authors (e.g., von Quadt et al., 2005, Kolb et al., 2013; Gallhofer et al., 2015; Knaak et al., 2016) came to the conclusion that the volcano-plutonic provinces of the entire ABTS belt were formed in response to a Late Cretaceous subduction process along the Eurasian active margin.

Unlike the Geticum, the Danubian imbricated nappe sequences are Moesia derived, developed by eastward thrusting during the Late Campanian-Maastrichtian (Berza et al., 1994) and they in turn were thrust over by the Getic and Supragetic units in the latest Cretaceous.

After the Cretaceous, the southern segment of the South Carpathians (East Serbian Carpathians, Gaudenyi and Milošević, 2023) were coevally affected by orogen-parallel and orogen-perpendicular extension, leading to the formation of numerous Oligocene-Miocene intramontane basins and the prolongation of the Pannonian Basin along the Morava Valley Corridor (Maţenco and Radivojević, 2012; Erak et al., 2017; Krstekanić et al., 2020).

In contrast to the numerous geological studies of the Carpatho-Balkanides, well-documented paleomagnetic results have been so far published only for its Romanian part. They supply evidence for large vertical axis clockwise rotations in the Banat area as well as in the Danubicum, N of the river Danube (Pătrăşcu et al., 1992, Panaiotu, 1998). These rotations are interpreted as due to bending around the NE corner of Moesia, since the latter did not change orientation, at least after the Eocene (e.g. van Hinsbergen et al., 2008).

The present study deals with the southward continuation of the Apuseni-Banat segment of the ABTS belt as well as the Danubicum. The new paleomagnetic constraints of the present study are intended to contribute to the better knowledge of the history of the tectonic development of the Carpatho-Balkanides.

2. Geological background

The studies carried out in the Timok Magmatic Complex (TMC) covered various aspects of the origin and evolution of the complex and established solid genetic links between magmatic processes and mineralization events. In this respect, the information based on stratigraphic relationships and high precision geochronology (Ar-Ar method: Clark and Ullrich, 2004; Lips et al., 2004,U-Pb zircon dating: e.g., von Quadt et al., 2005; Kolb et al., 2013; Knaak et al., 2016; Banješević et al., 2019; Velojić et al., 2023, Re-Os molybdenite dating: Zimmerman et al., 2008) was of supreme importance.

The TMC developed on a continental crust, and predominantly consists of extrusive volcanics and volcanoclastics that are associated with volcano-sedimentary and sedimentary rock series (Fig. 2a).

Prior to the volcanic activity, continuous platform carbonate sedimentation took place in the Early Jurassic – Lower Cretaceous time. A new sedimentation period of clastic character commenced with the Albian transgression related to oscillations of the depositional environment during Albian-/Cenomanian (Ljubović-Obradović et al., 2011). After a hiatus, the sedimentation re-started in the Turonian with basal conglomerate and continued with clastic to carbonate sediments (Oštrelj Formation) containing Helvetoglobotruncana helvetica, characteristic of lower to middle Turonian age (Ljubović-Obradović et al., 2011).

The magmatic activity started in the late Turonian and occurred in two phases: V1, dated as 90–83 Ma and V2 as 83–78 Ma (Fig. 2a). Both phases are characterized by predominant extrusive volcanism, shallow intrusions and volcanoclastics, which are associated with volcano-sedimentary and sedimentary rock series at places. The magmatic complex exhibits a steady decrease in age from east to west (Fig. 2a). This age progression away from the arc front toward the subduction trench can be interpreted as the sign of progressive steepening of the subducting slab (Gallhofer et al., 2015).

In the eastern segment, biotite-hornblende andesite (±dacite) compositions (Timok Andesite, Banješević, 2010, Banješević et al., 2019) are typical. They stratigraphically overlie Cenomanian siliclastic sediments or Turonian clastic/carbonate sediments. They belong to the V1 phase, which is subdivided into two sub-phases which systematically differ in their stratigraphic position, petrography, in age and in their link to mineralization. The older one, V1A (90–85 Ma) is substantially altered and mineralized, while the younger, V1B (85–83 Ma) is fresh and

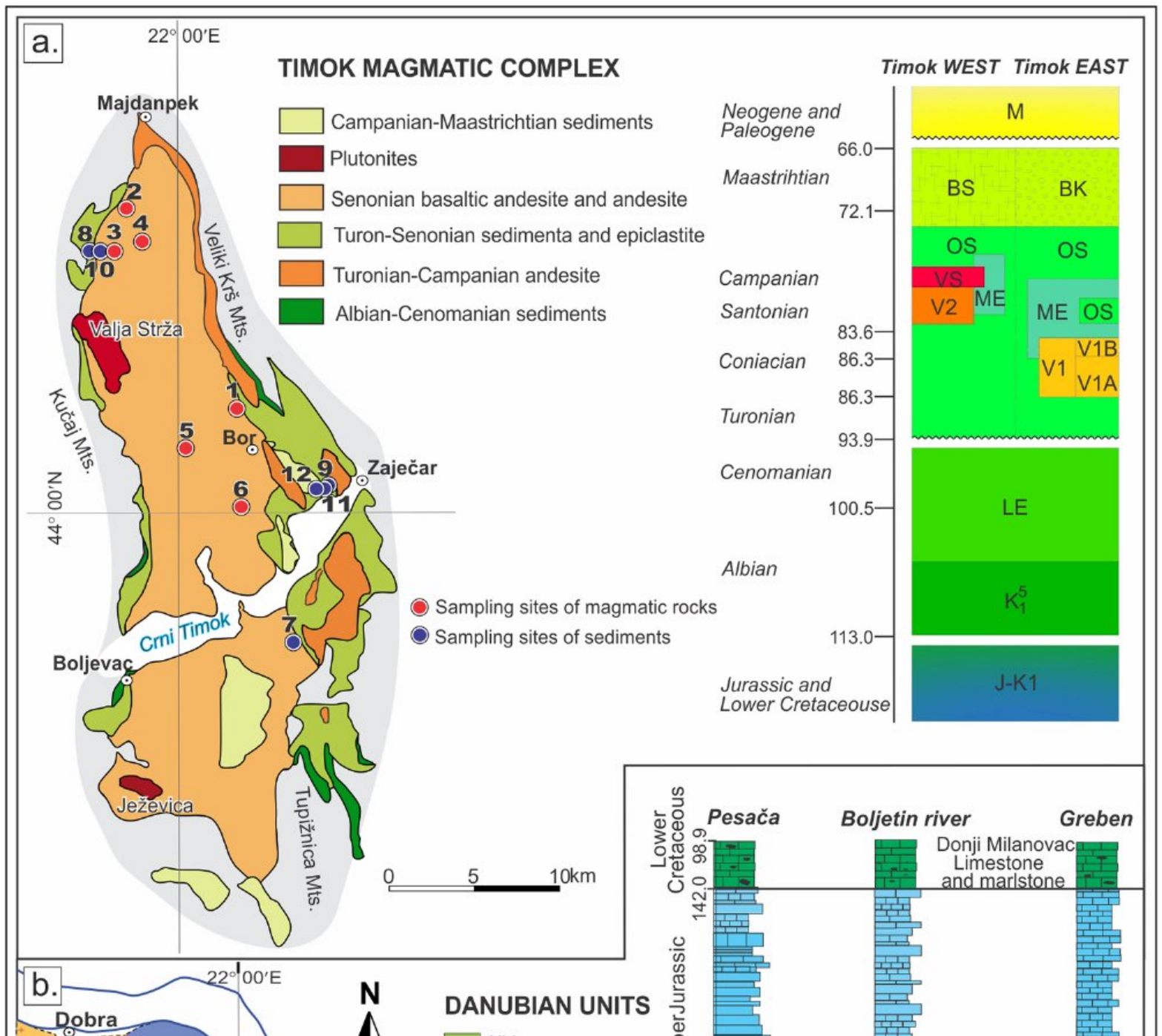

Fig. 2. Paleomagnetic sampling localities on geological maps accompanied by stratigraphic columns for the Timok area (Fig. 2a, based on Banješević, 2010; Ljubović-Obradović et al., 2011; Banješević, 2021) and for the Danubicum (Fig. 2b, based on Vasić et al., 1997, 1998). Key: LE – Lenovac Formation, OS – Oštrelj Formation, V1 – Timok Andesite, first volcanic phase, V1A and V1B – Timok andesite sub-phases, ME – Metovnica Epiclastite, V2 – volcanic second phase, VS – Valja Strž Plutonite, BS – Bukovo Formation, BK – Bor Clastic, M – Miocene sediments.

non-mineralized.

Towards the west, the hornblende-pyroxene andesites (V-1) grade to pyroxene andesite and basaltic andesite belonging to the V2 phase (Banješević, 2010) of 83–81 Ma (U/Pb zircon ages, von Quadt et al., 2002). They are predominantly emplaced as submarine extrusive volcanics, shallow intrusions and associated epiclastic rocks. Like the V1 volcanics, they are inter-layered with the sediments of the Oštrelj Formation and are at places covered by their epiclastic products (Đoršević, 2004; Banješević, 2010). In the westernmost part of the TMC a pluton of monzodiorite-granodiorite-gabbrodiorite composition (Valja Strž

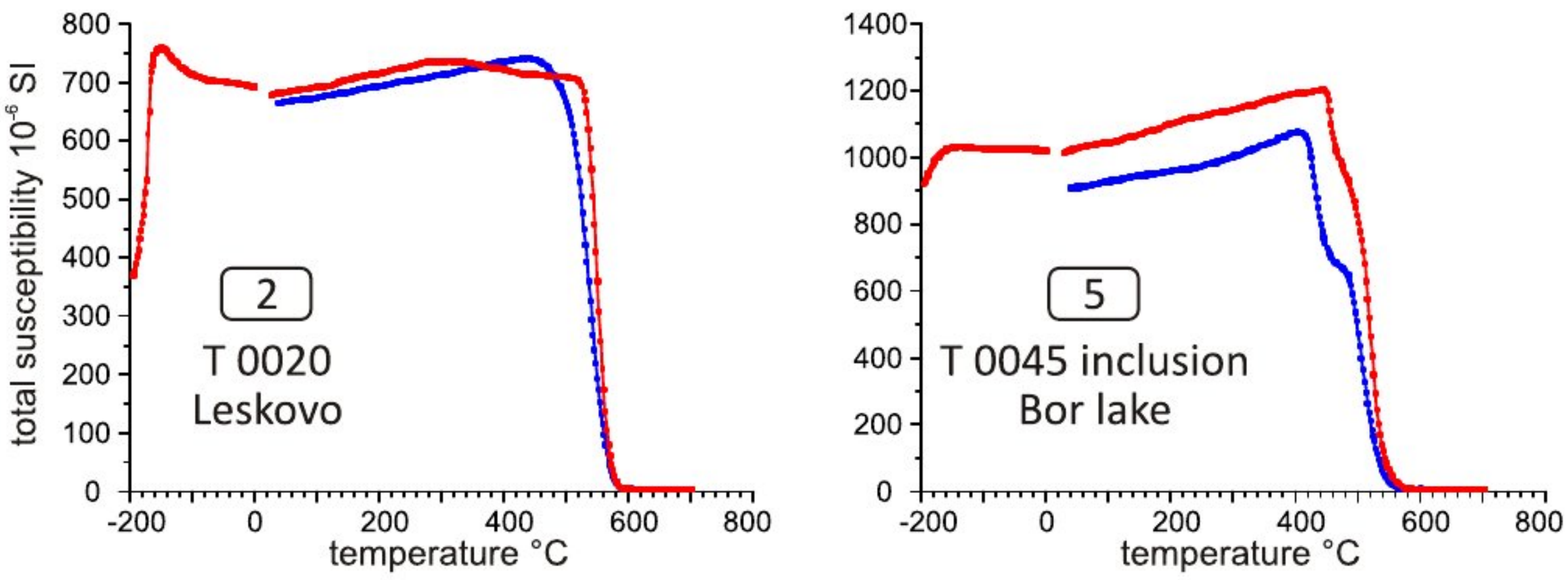

Fig. 3. Timok Magmatic Complex. Magnetite identified by low and high temperature characteristics of the susceptibility variation typical for V2 magmatic phase. Key: red curve, heating, blue curve, cooling (in argon atmosphere).

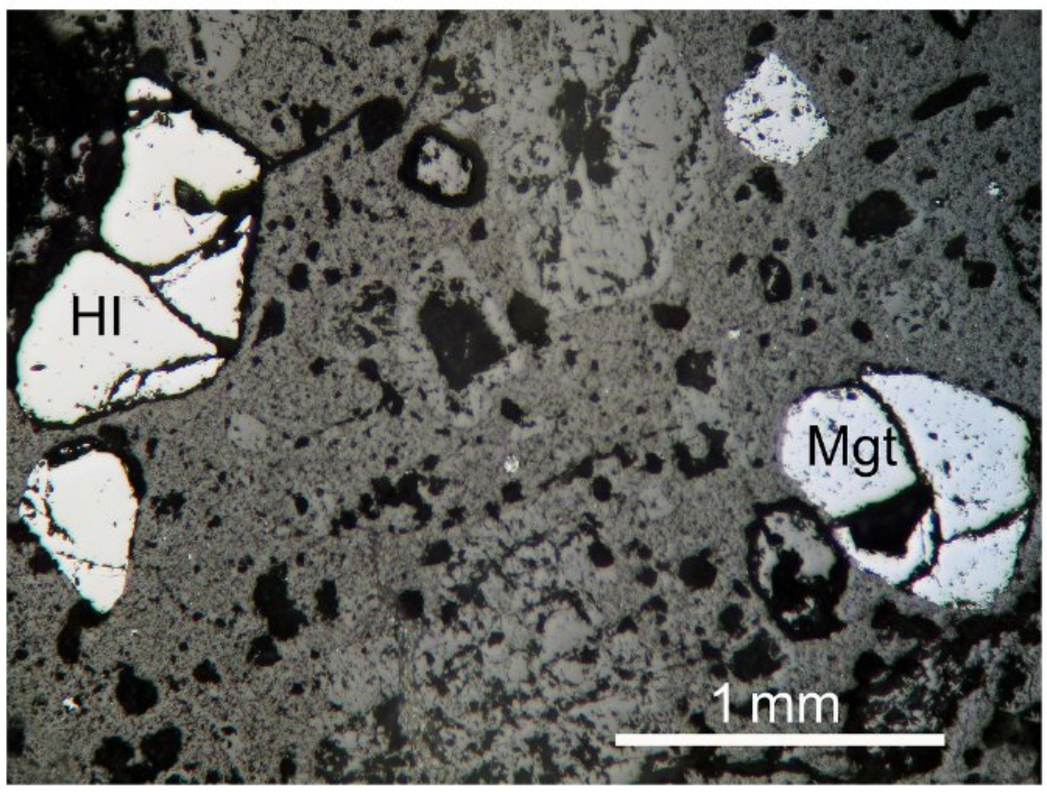

Fig. 4. Occurrence of hemoilmenite (HI) and magnetite (Mgt) in hornblende andesite from the Krivelj site (reflected light, air, //N, sample T0009b).

plutonite, Banješević, 2010) intruded the extrusive volcanics and surrounding sediments. The plutonic rock is dated at 83–78 Ma (von Quadt et al., 2002; Knaak et al., 2016).

In the upper Campanian - Maastrichtian, reef sedimentation took place in the western part of the Timok Magmatic Complex (Bukovo Formation, Ljubović-Obradović et al., 2011), while coarse-grained and regressive clastics were deposited in the eastern part, (Bor Clastic, Ljubović-Obradović et al., 2011). This was the period when the TMC was uplifted and its existence as an area of active volcanism/magmatism terminated (Banješević, 2021). New sedimentation cycles began only in the Miocene (Fig. 2a). These young deposits have recently been studied in drillholes (Rundić et al., 2019).

In the Danubicum, Jurassic and Lower Cretaceous sediments (Fig. 2b) lie discordantly over the Pre-Cambrian and Paleozoic basement. They are subdivided into three formations (Vasić et al., 1997): Siliciclastics and Limestone of Pesača (Lias and Lower Dogger), Boljetin Limestone (Middle Dogger-Tithonian), and the Lower Cretaceous Donji Milanovac Limestone (Fig. 2).

The siliciclastics and limestone of Pesača has clastic-carbonaceous character with the tendency of decreasing clastic content with age. The depositional environment was transitional and shallow-water marine.

The Boljetin limestone (Fig. 2b) deposited in deep-water with condensed sedimentation. It is subdivided into four members: 1. crinoidal limestones and Ammonitico rosso with hard ground; 2. red nodular limestones 3. red thin-bedded limestones with cherts; 4. red nodular limestones with cherts. Members 3 and 4 are characterized with concretional and bedded cherts, radiolarites and thick layers of calcarenites and calcruditcs made of material brought from shelf into the basin.

The Donji Milanovac limestone/marlstone formation comprises deep-water sediments with black cherts, deposited in reductive conditions (Berriasian - Lower Hauterivian) and shelf marls and marly limestone (Upper Hauterivian - Albian) indicating gradual shallowing.

3. Paleomagnetic sampling and laboratory measurements

The paleomagnetic samples were drilled with a gasoline powered drill and oriented in situ with a magnetic compass. The igneous rocks and the sediments under a metallic net were also oriented with a sun compass (sites T2-T6, localities D17, D19). Magnetic readings for the field orientation of the cores were corrected using IGRF-13 International Geomagnetic Reference Field model (Thébault et al. 2015). From the Timok Magmatic Complex Upper Cretaceous volcanic rocks (Fig. 2a, sites 1–6) and sediments (Fig. 2a, localities 7–12) were collected (133 independently oriented cores). From the Danubicum, Upper Jurassic (Fig. 2b, localities 13–18) and Lower Cretaceous (Fig. 2b, localities 19–21) limestones and marls were drilled (95 independently oriented cores). The cores were cut into standard size specimens. The laboratory processing started with the measurements of the natural remanent magnetization (NRM) in the natural state. It was followed by the measurements of the low field magnetic susceptibility.

Pilot samples were selected from each sample group, one specimen for alternating field (AF), the other for thermal demagnetization from the same sample. The pilot specimens were demagnetized in detail, till the NRM intensity was reduced practically to zero or when (rarely) instability set in. Possible changes in the magnetic mineralogy in thermally demagnetized specimens were detected by monitoring the magnetic susceptibility. Depending on the results of the pilot experiments, the rest of the samples from the respective groups were demagnetized either with AF or thermal method in several steps, allowing to define the components of the NRM. Each demagnetization curve (Zijderveld, 1967) was analyzed for linear segments (principal component analysis, Kirschvink, 1980). Statistical evaluation on locality/site level was based on Fisher (1953) method.

The instruments for the above laboratory measurements were JR-4 and JR-5A magnetometers (AGICO, Brno) KLY-2 kappabridge (AGICO, Brno), LDA-3A and Demag0179 AF demagnetizers (AGICO, Brno and Technical University Budapest, respectively), TSD-1 TH demagnetizers, (Schonstedt Instrument Company, Reston).

The magnetic minerals were identified in the igneous rocks by measuring the susceptibility as a function of the temperature and/or, by the thermal demagnetization of the 3-component isothermal remanent magnetization, (Lowrie, 1990), accompanied by susceptibility monitoring. For sediments, only the latter method was applicable. The instruments used were KLY-2 combined with CS-1 or CS-3 both from

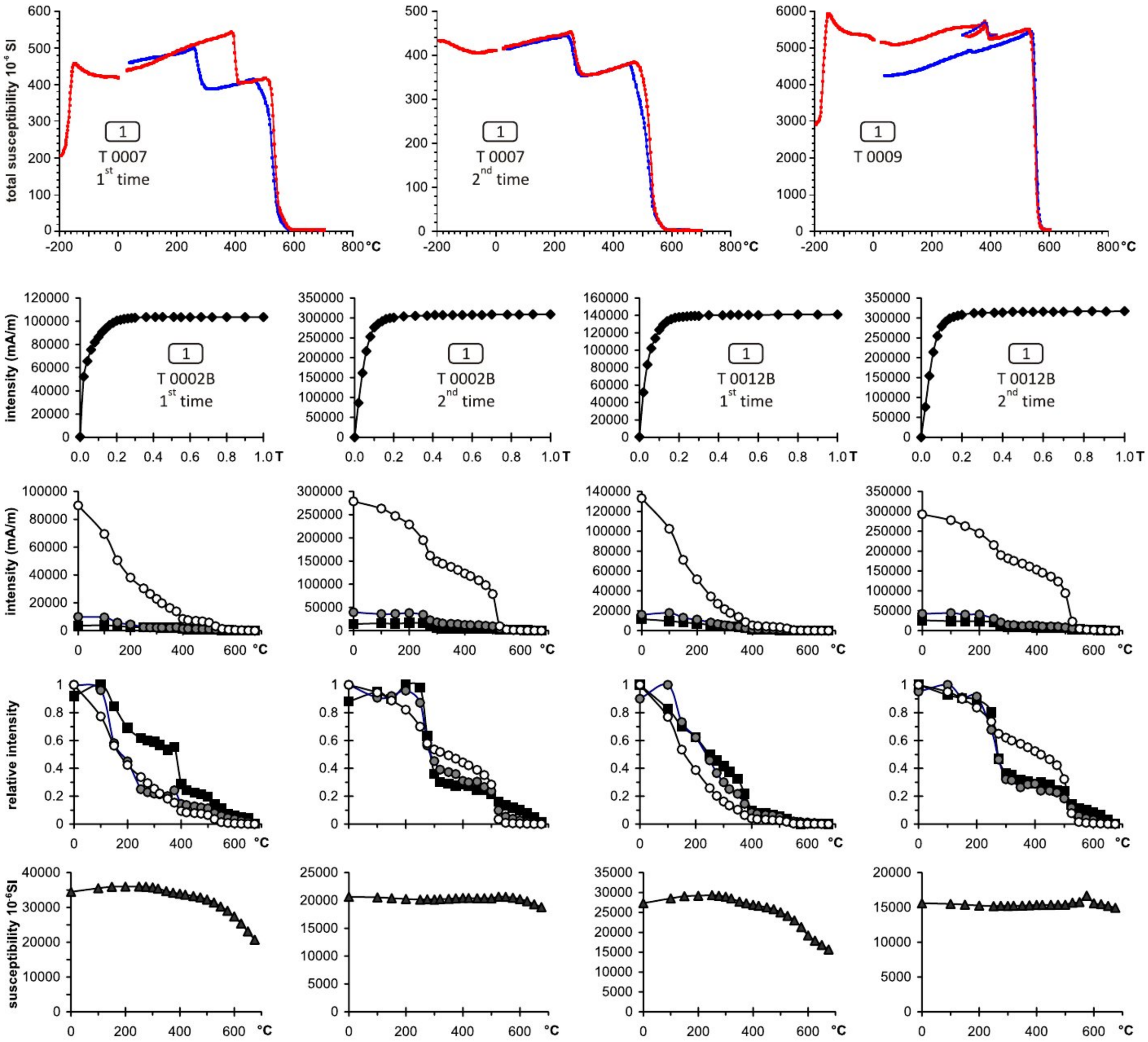

Fig. 5. Timok area, timocite. Identification of the magnetic minerals. First row: susceptibility vs temperature measurements Sample T0007 was heated (up to 700°C) and cooled twice. During the first heating, Curie points are at 410°C and 585°C, on cooling the first shifted to 300°C. During the second heating and cooling the Curie points are 300°C and 585°C, respectively. Sample T0009 was treated differently: on first heating (up to 420°C) the Curie point is 410°C, on controlled cooling (down to 310°C.) it stays there. During a second heating (up to 600°C) it stays at 410°C, while on cooling from 600°C it drops to 300°C. From second to last row: results of the Lowrie experiment showing: fast acquisition of the IRM, followed by the results of stepwise thermal demagnetization of the 3-component IRM, next row shows the normalized curves, while the last one the results of the susceptibility monitoring. The dominance of hemoilmenite is clear from the first runs, while the second documents the formation of magnetite and hematite on heating. Key: The components of the IRM were acquired in fields of 1.0 T (squares), 0.36 T (full circles) and 0.12 T (open circles).

AGICO (Parma et al., 1993; Hrouda, 1994). The isothermal remanent magnetization (IRM) acquisition experiments were made either with a Molspin Pulsemagnetizer (Molspin) or a MMPM10 pulse magnetizer (Magnetic Measurements).

Mineralogical investigations were also carried out on paleomagnetic specimens from Krivelj (Fig. 2a, site 1), using the same method, the same equipment and the same analysis conditions as Luković et al. (2021). They determined the composition and chemical homogeneity of some hemoilmenites from the TMC, using scanning electron microscopy with energy-dispersive spectrometer (SEM-EDS). The paleomagnetic specimens from Krivelj (Fig. 2a, site 1) were not only studied in the natural state but also after the thermal demagnetization of the paleomagnetic analysis, in order to check if phase transformations and/or exsolution took place during heating. This investigation was carried out in the following way. A powdered sample of hemoilmenite was first embedded in epoxy resin and polished in several steps using diamond pastes of 15, 9, 6, 3 and 1 μm. The SEM examination of the prepared samples, based on the back-scattered electron (BSE) images could not reveal differences in the pre and post-heating state of the Krivelj hemoilmenite.

4. Results

4.1. Magnetic mineralogy

In the paleomagnetic samples from the TMC magnetite is the typical magnetic mineral (Fig. 3), which is quite stable on heating. Exception is

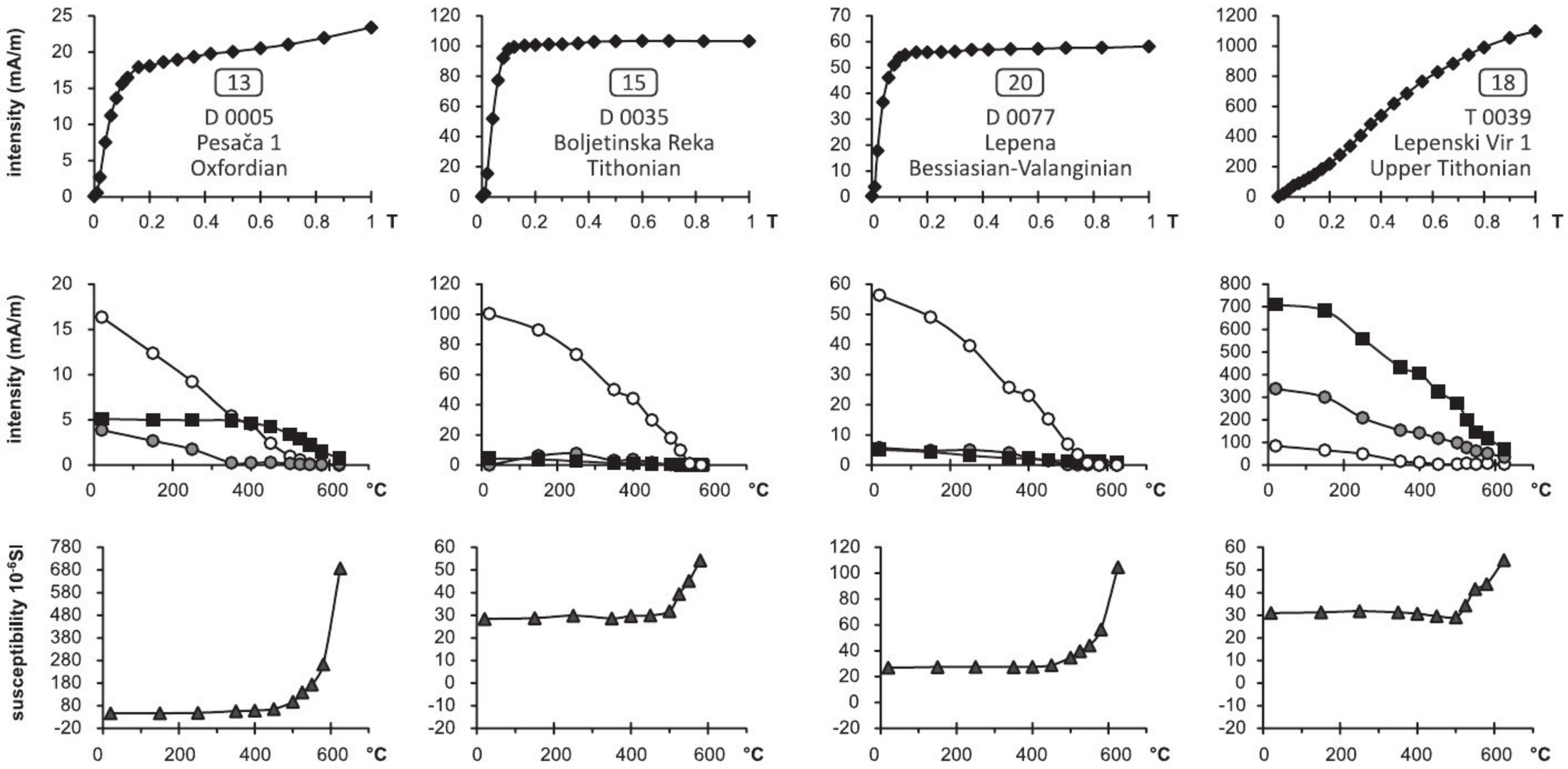

Fig. 6. Danubicum. Identification of the magnetic minerals. Lowrie experiment showing: acquisition of the IRM (first row), the results of stepwise thermal demagnetization of the 3-component IRM (second row) and the results of the susceptibility monitoring (last row). Key: see Fig. 5.

the hornblende andesite (variety *Timocite*) of the V1B sub-phase which contains magnetite, but also hemolimenite (or *ferrian ilmenite*), which is an intermediate member of the hematite-ilmenite solid solution (Luković et al., 2021). Hemoilmenite is present in all samples, and its content in relation to magnetite varies in the range from half to almost the same abundance as magnetite. Most of the Fe-(Ti) oxides occur in anhedral to subhedral grains from 0.2 to 1.5 mm in size, but magnetite sporadically also forms coarser grains up to 4 mm in size. Magnetite and hemoilmenite frequently show mutual intergrowths, but they also occur in separate grains (Fig. 4). Both minerals are free of exsolutions.

Magnetite is identified by both low and high temperature features of the susceptibility versus temperature curves. Hemoilmenite on first heating exhibits a Curie-point which is invariably close to 410°C (Fig. 5, uppermost row). After the first heating run (up to 700°C), the Curie temperature of 410°C drops to around 300°C and remains there on repeated heating-cooling (Fig. 5, uppermost row, T7). Lowrie (1990) experiments document fast saturation of the IRM and the three component IRM reveals a dominant soft mineral with steadily decreasing intensity on thermal demagnetization up to about 400°C and a small remnant persisting till the Curie point of magnetite (Fig. 5, T2 and T12). The hard component clearly shows a significant intensity drop at about 400°C (Fig. 5, 4th row). On repeated heating the intensity of all three components increase dramatically, while the break in the intensity curve shifts from 400°C to about 300°C. During heating hematite is produced, which is clearly identified by the total decay of the hard component by 680°C. All these features point to hemoilmenite as the "partner" magnetic mineral of the magnetite.

The magnetic minerals in the Danubicum are magnetite, sometimes accompanied by a magnetically hard component, except locality 18, where the hard component is dominant, which, however is decaying well before the Curie point of the hematite (Fig. 6).

4.2. Paleomagnetic directions

From the Timok Magmatic Complex, most of the magmatic and the sedimentary rocks are characterized by composite NRM. Samples from the former were mostly demagnetized thermally, while the components of the NRM in the sediments were fairly well revealed from the stepwise AF demagnetization curves (Fig. 7). The site/locality mean directions were calculated from the components decaying towards the origin, except site 1 (Table 1). In this case the component of normal polarity, residing in hemoilmenite and eliminated by about 400°C, was regarded as the characteristic magnetization (ChRM), since the reversed polarity component, connected to magnetite was often very small (Fig. 7, T9A) and noisy. Due to the above effect, the inclination of the component demagnetized by 400°C is somewhat shallower than the rest of the studied sites/localities from the Timok area (Table 1).

The Upper Jurassic and the Lower Cretaceous sediments from the Danubicum, mostly demagnetized by AF method, have practically single component NRM, which decays completely by the Curie point of magnetite (Fig. 7). During heating the susceptibility remains stable, pointing to magnetite as the carrier of the NRM. Hematite, when present in some specimens must have no or very little contribution to the NRM, as the AF method always demagnetizes the NRM by 50 mT.

5. Discussion

The paleomagnetic results of the present study provide evidence for a moderate post-Cretaceous CW rotation of the Timok Magmatic Complex (Fig. 8). This is based on five fresh magmatic sites postdating the ore mineralization, which caused the alteration of the igneous rocks belonging to V1A phase, and the pre-tilting magnetizations of two sedimentary localities (Table 1).

The carrier of the NRM in the above magmatic rocks is magnetite, except in the timocite (site 1), where hemoilmenite is often more important contributor to the NRM than magnetite (Fig. 7, specimen T9A). Hemoilmentite was positively identified also by mineralogical studies, which revealed the presence of 0.2–1.5 mm diameter individual grains of hemoilmenite, spatially associated (Fig. 4) or sometimes intergrown with magnetite. Both the magnetite and hemoilmenite were free of exsolutions. The magnetite contained only traces of titanium (Luković et al., 2021), also proved by our magnetic experiments, which detected Curie points of pure magnetite (Fig. 5, first row). However, the composition of the hemoilmenite estimated by mineralogical and magnetic methods are different. The dependence of the unit cell volume with composition, obtained by the method of X-ray diffraction, Luković et al.

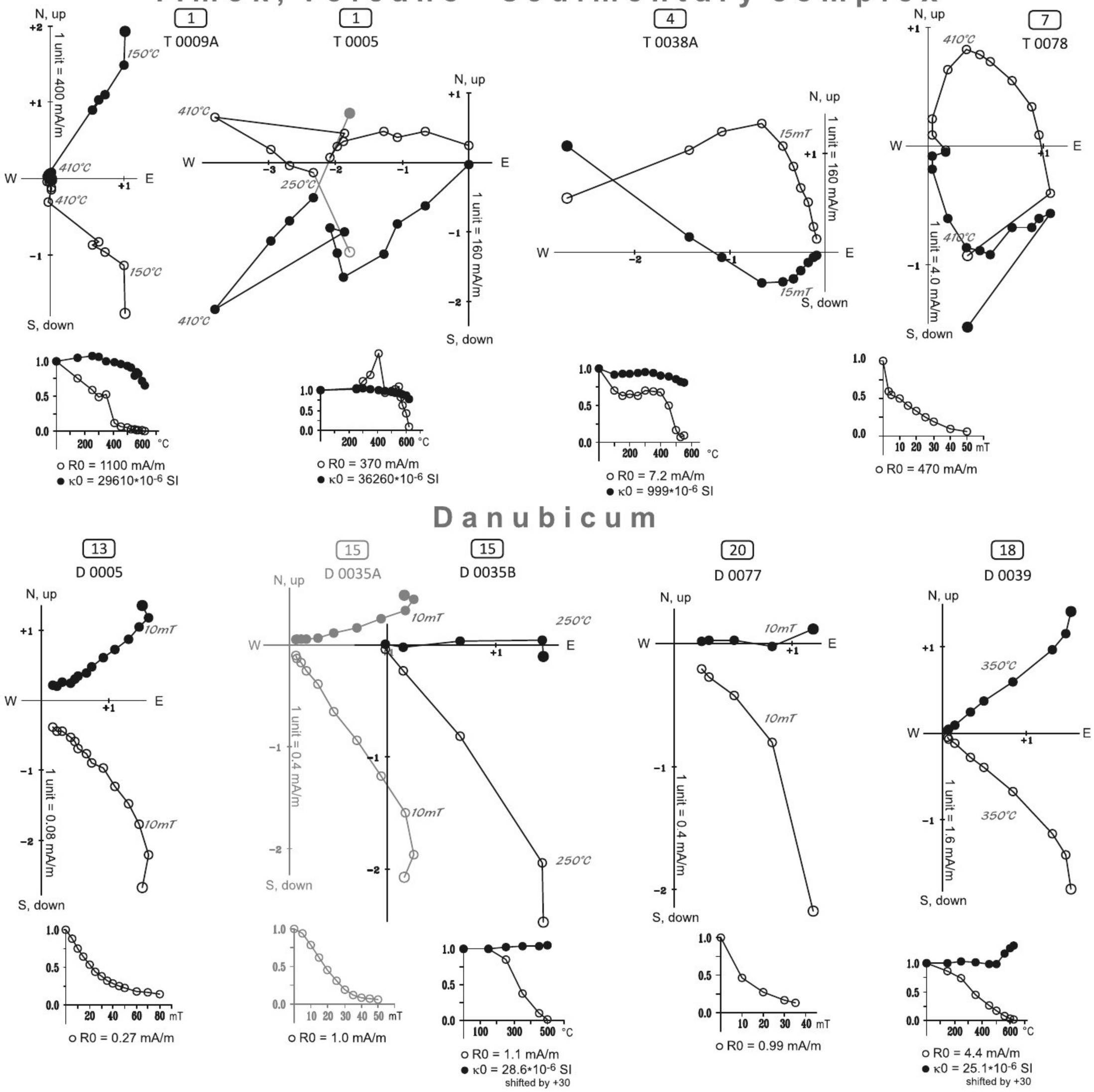

Fig. 7. Timok Magmatic Complex, Upper Cretaceous magmatic and sedimentary rocks and Danubicum, Upper Jurassic and Lower Cretaceous sediments. Typical demagnetization curves (Zijderveld diagrams). Note that in timocite T0009 exhibits practically one component, connected to hemoilmenite while T0005 shows two components, one is up to 410°C and N polarity (connected to hemoilmenite), afterwards up to 600°C R polarity, connected to magnetite Key: Zijderveld diagrams (Zijderveld, 1967) in geographic system. In case of AF demagnetization they are accompanied by intensity (circles) versus demagnetizing field diagrams, and by NRM intensity (circles)/susceptibility (dots) vs. temperature diagrams, when the method is thermal (TH) demagnetization. In the Zijderveld diagrams full dots are the projections of the NRM vector onto the horizontal; circles: into the vertical.

(2021) implies that this solid solution member contains 53 mol% ilmenite in average. Similar composition is confirmed by the SEM-EDS analysis of the paleomagnetic specimens (53±1 mol% ilmenite). This corresponds to a Curie point of 200°C, which falls in the field of natural ferromagnetic hemoilmenites (Nagata, 1961). The magnetic experiments carried out with different methods (Curie–point measurements, stepwise thermal demagnetization of the IRM as well as the NRM (Figs. 5 and 7) all confirm that the Curie point of the hemoilmenite in all paleomagnetic samples is about 400°C on the first heating run, indicating a composition of about 30 mol% of ilmenite (Nagata, 1961). In the course of our experiments, the composition of the hemoilmenite changes after the first heating run from 400°C to 300°C and stabilizes there as documented by repeated heating (Fig. 5). Unlike the magnetic experiments the SEM-EDS analysis of the heated samples did not suggest textural transformations (e.g. exsolution).

The results of the magnetic experiments can be explained by the model put forward by Prèvot et al. (2001). This model envisages the co-existence and interaction of three main phases of somewhat different

Table 1
Summary of site/locality mean palaeomagnetic directions based on the results of principal component analysis (Kirschvink, 1980) except site T3 where combination of stable end points and demagnetization circles was used (McFadden and McElhinney, 1988).

	Locality	Lithology	Age	Lat (°) Lon (°)	n/ no	D (°)	I (°)	k	α_{95}(°)	Dc (°)	Ic (°)	k	α_{95}(°)	Dip	Paleo lat (°)	Pole lat (°)	Pole long (°)	δp (°)	δm (°)
Timok magmatic complex																			
T1	Mali Krivelj, quarry T0001–013	hornblende biotite andesite (Timozite)	84.66±0.5 Ma	44°08' 22°05'	7/ 13	36.2	25.0	64.8	7.6	36.2	25.0	64.8	7.6		13.1	46.2	145.8	4.4	8.2
T2	Leskovo, road cut T0014–023	andesite	83 – 78 Ma	44°19' 21°56'	9/ 10	192.4	−41.7	100.1	5.2	192.4	−41.7	100.1	5.2		24.0	67.3	171.4	3.9	6.3
T3	Jasikovo, Jagnjilo stream, T0024–034	andesite, small intrusion	83 – 78 Ma	44°17' 21°54'	8/ 11	148.7	−43.5	90.2	6.1	178.2	−55.7	90.2	6.1	99/27	36.3	81.9	212.5	6.2	8.7
T4	Jasikovo T0035–044	andesite dyke	83 – 78 Ma	44°17' 21°57'	8/ 10	224.3	−63.3	165.3	4.3	224.3	−63.3	165.3	4.3		44.9	58.9	95.0	5.4	6.8
T5	Bor lake, quarry T0045–064	basalto andesite lava flow	83 – 78 Ma	44°06' 22°00'	15/ 20	204.0	−42.0	104.6	3.8	204.0	−42.0	104.6	3.8		24.2	62.1	149.5	2.8	4.6
T6	Brestovac T0065–076	albite-trachyte dyke	81.79 ±0.5–82.27 ±0.35 Ma	44°03' 22°05'	11/ 12	11.6	42.9	58.8	6.0	11.6	42.9	58.8	6.0		24.9	68.7	172.1	4.6	7.4
T7	Strmen, railway cut T0077–088	marl	Lower to Middle Turonian	43°56' 22°08'	10/ 12	153.5	−43.2	36.2	8.1	215.8	−47.9	36.2	8.1	99/54	28.9	57.9	127.8	6.9	10.6
T8	Jagnjilo spring T0089–100	layered marls and siltstone	Lower to Middle Turonian	44°17' 21°53'	7/ 12	14.1	41.5	101.6	6.0	34.1	34.3	101.6	6.0	99/27	18.9	51.9	142.7	4.0	6.9
T9	Donja Bela reka T0101–110	epiclastite	Lower to Middle Turonian	44°04' 22°11'	0/ 10									99/12					
T10	Jasikovo T0111–121	layered marls	Lower to Middle Turonian	44°17' 21°55'	0/ 11									105/34					
T11	Ostrelj T0127–127	layered marls and siltstone	Lower to Middle Turonian	44°04' 22°11'	0/6									242/38					
T12	Ostrelj T0128–133	epiclastite	Lower to Middle Turonian	44°04' 22°11'	0/6									247/48					
Danubicum																			
D13	Pesača 1 D 0001–007	grey siliceous marl	Oxfordian	44°36' 22°00'	6/7	55.8	42.8	129.1	5.9	33.3	45.3	129.1	5.9	309/23	24.8	41.2	116.5	4.5	7.3
D14	Pesača 3 D 0022–027	red limestone	Oxfordian	44°36' 22°00'	5/6	63.5	48.2	78.7	8.7	22.1	52.2	78.7	8.7	307/33	29.3	38.3	106.5	7.5	11.4
D15	Boljetinska reka D 0028–038	grey pelagic limestone	Tithonian	44°32' 22°02'	11/ 11	77.7	55.3	218.7	3.1	76.3	67.3	218.7	3.1	261/12	35.9	32.3	91.5	3.1	4.4
D16	Lepenski Vir2 D 0046–062	red and grey limestone	Tithonian	44°34' 22°01'	12/ 17	68.1	40.8	170.2	3.3	44.0	44.8	117.2	4.0	317/23, 313/25, 306/32	23.4	31.5	109.2	2.5	4.1
D17	Pesača 2 D 0008–021	red-purple limestone	Tithonian	44°36' 22°01'	11/ 14	54.5	54.0	137.2	3.9	342.3	59.1	49.0	6.6	286/45 286/38 281/54	34.6	47.6	106.2	3.8	5.5
D18	Lepenski Vir1 D 0039–045	red nodular limestone	Upper Tithonian	44°33' 22°02'	7/7	63.4	33.7	285.3	3.6	60.3	49.4	285.3	3.6	255/16	18.5	31.6	116.9	2.3	4.1
D19	Lepenski Vir3 D 0063–075	grey limestone	Berriasian	44°39' 22°01'	9/ 13	71.1	12.1	47.0	7.6	39.8	54.1	47.0	7.6	284/58	34.7	58.2	116.3	7.5	10.6
D20	Lepena D 0076–086	grey limestone	Berriasian-Valanginian	44°34' 22°01'	9/ 11	94.6	38.4	97.0	5.3	59.5	71.6	97.0	5.3	294/39	56.4	51.7	72.3	8.1	9.2
D21	Greben D 0087–095	grey limestone	Barremian-Aptian	44°31' 22°04'	7/9	43.6	59.1	39.6	9.7	40.4	63.8	39.6	9.7	242/5	45.4	61.7	95.7	12.2	15.4

Key: Lat.N, Lon.E: Geographic coordinates (WGS84) measured by GPS, n/no: number of used/collected samples (the samples are independently oriented cores); D, I (Dc, Ic): declination, inclination before (after) tilt correction; k and α95: statistical parameters (Fisher, 1953); Paleo lat: paleolatitude; Pole lat and Pole long: coordinates of the paleopole; δm, δp: statistical parameters of the palaeomagnetic pole. U/Pb age for locality 1: 84.66±0.5 and for locality 6: 81.79±0.5–82.27±0.35 (Von Quadt et al., 2002). Formations: 1 (V1B subphase): Timok Andesite. 2–6 (V2 phase): Ježevica andesite, Osnić basaltic andesite. 7–8, 10–12: Ostrelj Formation. 9: Metovnica Epiclastite.

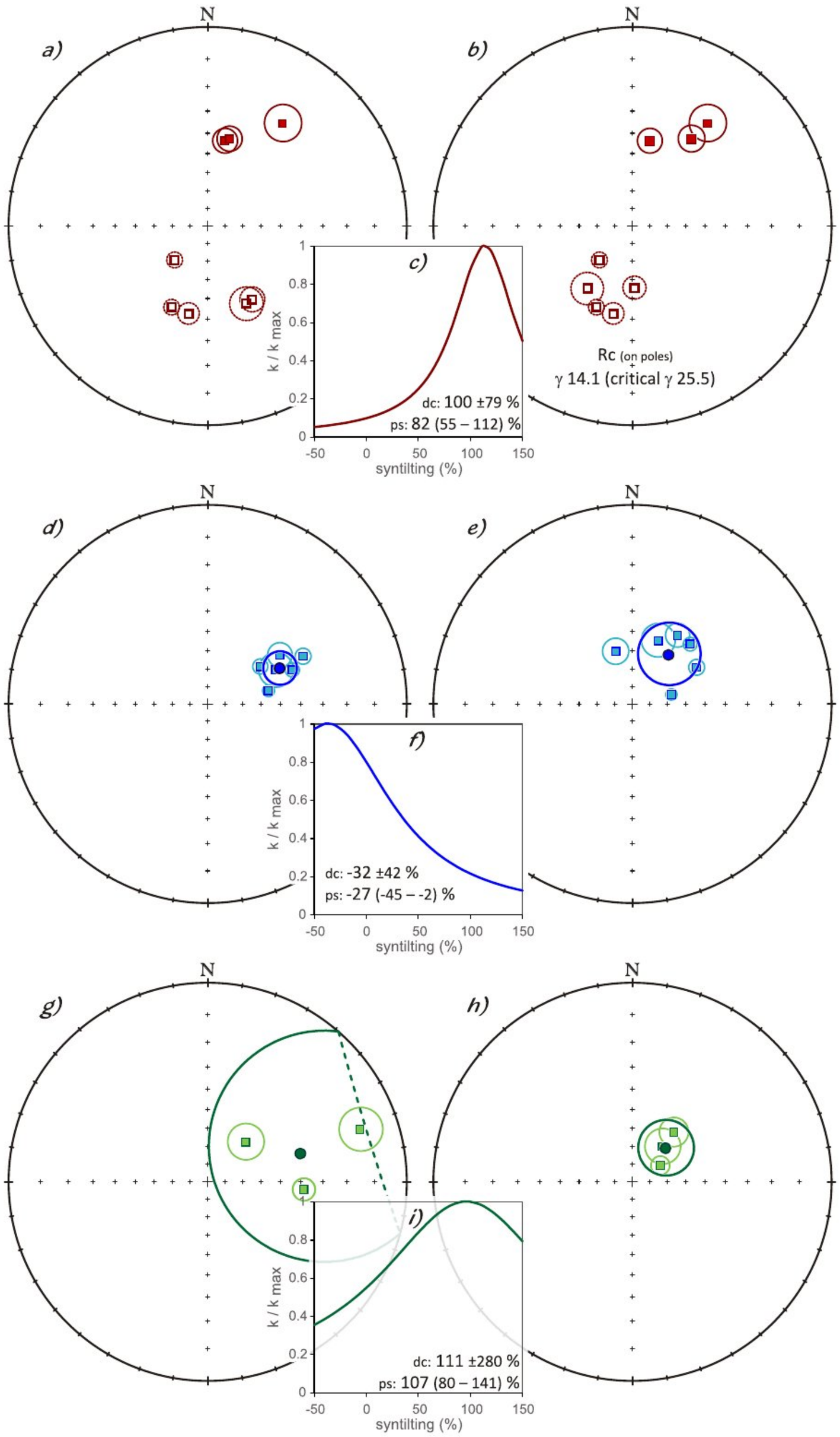

Fig. 8. Between locality tilt test for the Timok Magmatic Complex (a-c) for the Upper Jurassic of the Danubicum (d-f) and for the Lower Cretaceous of the Danubicum (g-i). The results are plotted before (left side stereoplots) and after (right side stereoplots) tilt corrections. The results of the incremental tilt tests are shown in-between, documenting significant improvement on back-tilting for the Timok Magmatic Complex (a-c), and the negative character for the Upper Jurassic of the Danubicum (d-f). The Direction correction test (Enkin, 2003) is indeterminate for the Lower Cretaceous of the Danubicum (g-i), but the parametric simulation fold test (Watson and Enkin, 1993) is significantly positive. Key to the incremental tilt test: dc: direction-correction tilt test (Enkin, 2003); ps: parametric simulation fold test (Watson and Enkin, 1993) with 95 % confidence limit, circular standard deviation of the dip was 8°. On stereonet: Rc: classification of reversal test (McFadden & McElhinney, 1990) carried out on poles.

Table 2
Summary of the overall mean paleomagnetic directions before and after tilt corrections, results of direction correction (dc), parametric simulation (ps) tilt/fold (Enkin, 2008 and Watson and Enkin, 1993, respectively) and reversal (McFadden and McElhinney, 1990) test and paleomagnetic poles with statistical parameters. Localities and sites T1-T8: Table 1, localities D13-D19: Table 1, localities B4-B6, B8A and B8B: Panaiotu et al. (2012). Common mean direction test based on McFadden and McElhinney (1990) between localities D13-18 (this paper) and B4-B6, B8A, B8B (Panaiotu et al., 2012): Classification B, γ8.9° (critical γ12.2°).

		PALEOMAGNETIC DIRECTION								FOLD/TILT & REVERSAL TEST	PALEOMAGNETIC POLE								
											Based on localities				Based on samples				
	N	D°	I°	k	α_{95}(°)	D_C°	I_C°	k	α_{95}(°)	Optimal untilting, classification	Lat. (°)	Long. (°)	K	A95 (°)	n	Lat. (°)	Long. (°)	K	A95 (°)
Timok Magmatic Complex																			
Timok (T1-T8)	8	10.3	45.6	14.5	15.1	**24.8**	**45.0**	26.3	11.0	dc 100 ± 79, positive ps 82 (55–112) Rc, γ14.1, critical γ25.4	64.3	143.9	23.4	11.7	75	65.0	144.9	21.4	3.6
Danubicum																			
Danubicum Serbian shore of Danube (D19-D21)	3	73.1	38.1	7.6	48.2	**44.6**	**63.4**	67.8	15.1	dc 111 ± 280, indeterminate ps 107 (80–141)	58.5	93.5	38.3	20.2	25	58.5	91.5	21.4	6.4
Danubicum Serbian shore of Danube (D13-D18)	6	**63.6**	**46.1**	66.1	8.3	36.4	56.1	17.8	16.3	dc −32 ± 42, negative	37.4	107.7	66.2	8.3	52	37.2	106.2	44.3	3.0
Danubicum Serbian + Romanian shore of Danube (D13–18 + B4–6 & 8A-B)	12	**69.3**	**48.2**	49.0	6.3	58.3	52.7	9.4	14.9	dc 10 ± 21, negative	34.6	102.2	42.1	6.8	133	31.7	101.7	26.9	2.4

Key as for Table 1, but N is the number of localities. For localities B4-B6, B8A and B, pole statistics based on samples by Cox (1970) method.

composition, degree of ordering and the direction of the alignments to the applied magnetic field of three phases of a hemoilmenite crystal. The one with the Curie point about 300°C can be in the nucleus of the system, which is a fully ordered crystallographic domain. The Curie-point of about 400°C corresponds to the iron enriched domain. The latter is surrounded by a disordered crystallographic domain, with Curie point of 200°C, expected for the ilmenite content of the SEM-EDS analysis. The transition from an iron-rich phase to the crystallographically fully ordered stable hemoilmenite is clearly documented by our magnetic experiments, while the crystallographically disordered dominant phase of the hemoilmenite grains is magnetically mute.

The Danubicum, which offers only sediments for paleomagnetic investigation, was sampled along the Serbian shore of the river Danube (Fig. 2b). From this unit, all localities provided results with excellent or good statistical parameters (Table 1). The Jurassic localities form a tight cluster before tilt corrections, indicating about 64° CW vertical axis rotation, while exhibit a large scatter on back-tilting (Fig. 8). The Lower Cretaceous locality mean directions are widely scattered before and grouping tight after tilt corrections. However, their overall-mean direction has a quite large α_{95}, due to the low number (three localities) of entries (Fig. 8). For this reason, the angle of the CW rotation implied by the Cretaceous localities is taken as a proof for the CW rotation but not considered as constraining the magnitude.

Earlier, Upper Jurassic sediments had been studied from the Romanian side of the river Danube (Panaiotu et al., 2012). They also found that the paleomagnetic signals were of post tilting age (probably Aptian). The overall mean paleomagnetic direction suggested about 75° vertical axis CW rotation, yet the angular distance between results from the Romanian and Serbian sides of the river (γ8.9, critical γ12.2, classification B, McFadden and McElhinney, 1990) permits to combine them. The result is a statistically well-constrained paleomagnetic overall-mean direction pointing to 69° vertical axis CW rotation (Table 2) after the Aptian.

The other target of the present study, the Timok Magmatic Complex, belongs to the Getic unit and represents one of the five Cu-Au mineralized area of the ABTS segment of a Late Cretaceous magmatic arc (Gallhofer et al., 2015). The formation of the arc is related to subduction and the mineralization is attributed to temporary stress release at discrete segments. This affected earliest the Srednogorie segment (87–92 Ma), followed by the Timok segment (81–88) and last the Banat–Apuseni sector (72–83). Such an along strike pattern is less obvious in the age of the accompanying igneous rocks, for each sector encompasses similar age ranges with almost 90 % of radiometric data falling between 70 Ma and 90 Ma (Gallhofer et al., 2015).

Earlier published paleomagnetic studies provide data for Upper Cretaceous igneous rocks from all segments, except the TMC. Those representing three areas of the Srednogorie sector (Nozharov and Veljović, 1974, Nozharov et al., 1977, Nozharov and Petkov, 1984), can be interpreted in terms of no or maximum 10° CCW vertical axis rotation after the Cretaceous (Fig. 9). This interpretation was confirmed by Kruczyk et al. (1990), based on the post-tilting magnetization of Jurassic sediments, acquired during the ore mineralization. Nozharov and Veljović (1974) continued the study of the ABTS belt towards the NW and documented about 19° CW rotation for Upper Cretaceous lava rocks close to the Serbian-Bulgarian boundary (Fig. 9). As we travel further to the north, the Timok segment of the present study shows about 25°CW rotation. The angle of the CW rotation reaches about 90° in the Apuseni-Banat sector of the ABTS magmatic arc (Fig. 9).

The paleomagnetic data now available permit to test them against the changing general strike of the studied areas (Fig. 10). The test documents that the Moesian orocline is a progressive arc. As the slope of the correlation diagram is 0.6, the present arc must have formed from a non-linear feature i.e. the concept of the E-W orientation at the time of the magmatic activities must be abandoned. A model, which calculates with a Cretaceous subduction zone which is generally E-W oriented in the S sector, followed by NNW–SSE oriented ABT sectors is the likely solution

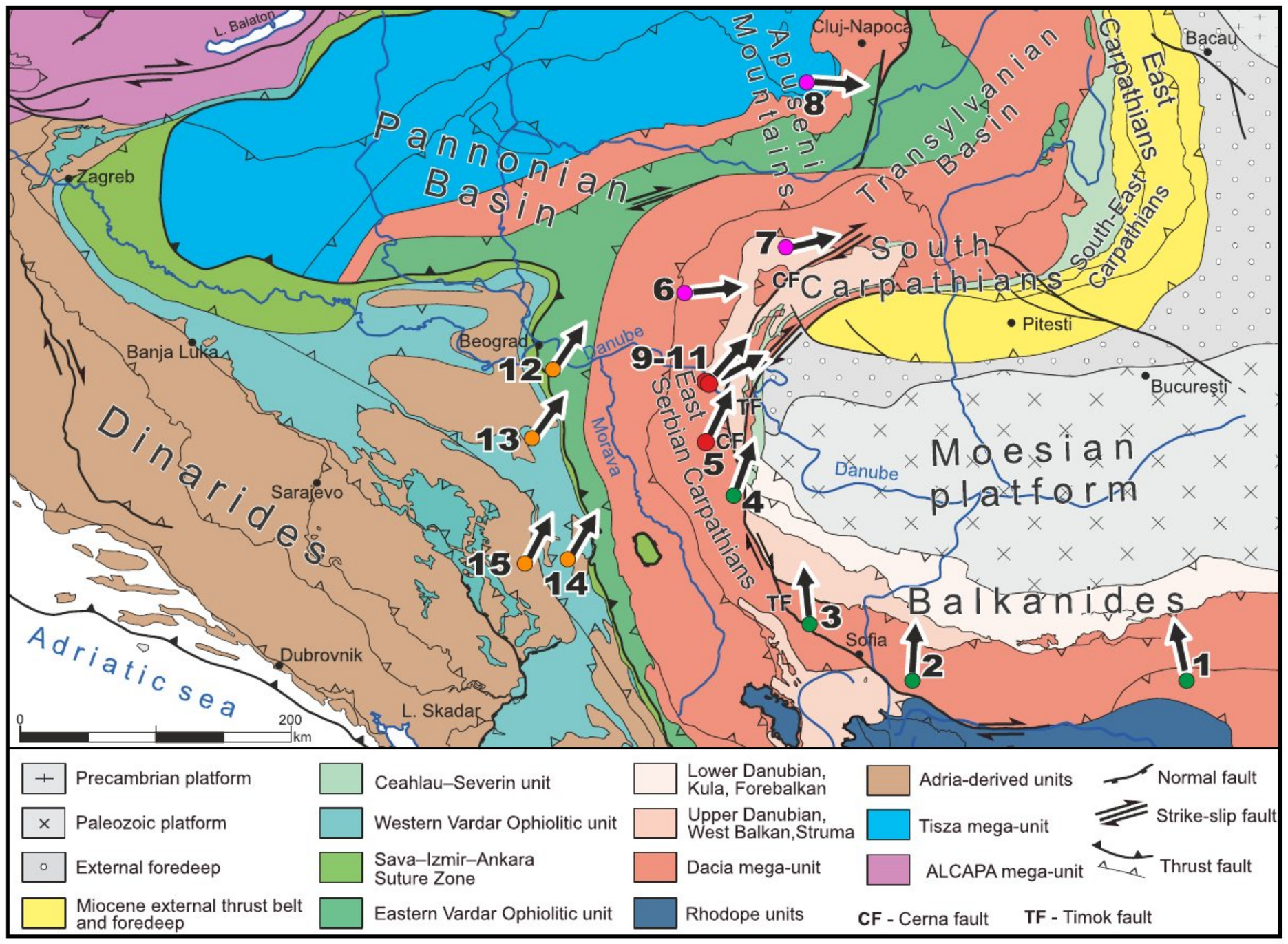

Fig. 9. Paleomagnetic declinations constraining the vertical axis rotations in the Apuseni-Banat-Timok-Srednogorie Late Cretaceous magmatic arc (1–8), and in the Late Jurassic-Early Cretaceous of the Upper Danubicum (9–11), in comparison with data from the Eastern (12) and Western (13–14) Vardar Zones as well as from the Drina–Ivanjica unit (15) pointing to about 30° vertical axis CW rotations after 20 Ma (probably between 20 and 17 Ma). References: 1–4 (Nozharov and Veljović, 1974, Nozharov et al., 1977, Nozharov and Petkov, 1984), 5, 10, 11 (present study), 9 (Panaiotu et al., 2012), 6–8 (Pătrăşcu et al., 1990, 1992, 1994), 12–14 (Márton et al., 2022), 15 (Velki et al., 2023). Map by Schmid et al. (2020).

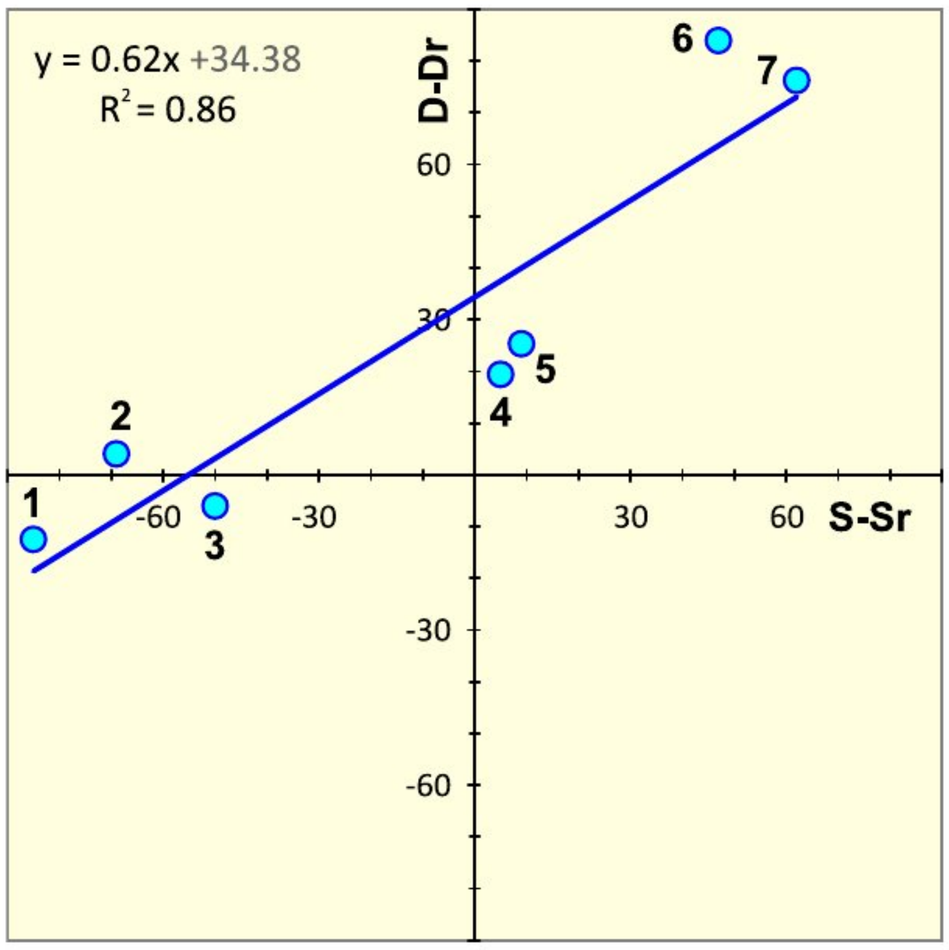

Fig. 10. Strike test plot for the circum Moesian orocline, documenting that it is a progressive arc (e.g. Pastor-Galán et al., 2011). The diagram is showing declination deviations relative to fold axis deviations from reference values, which are Dr=0° (reference declination) and Sr=0° (reference strike). D and S are the overall mean declinations and the general tectonic trends, respectively at several areas distributed along the orocline. The slope of regression line is 0.6, significantly different (t=5.5, t99=3.4) from the zero slope (meaning primary arc) and also from 1.0 (meaning secondary orocline bending of an originally straight structure). Locality/site numbers referring to Fig. 9.

(Fig. 11)

In a short communication Neubauer (2015) gives a reconstruction for south-eastern Europe for 83 Ma (Santonian-Campanian) which locates the ABTS belt south of the Severin–Ceahleu branch of the Alpine Tethys. The belt runs E-W for a while then becomes sub-parallel with a NW-SE oriented segment of the already closed part of the Vardar ocean. It is reasonable to assume that apart from the Srednogorie segment, the belt started to change orientation towards NNW. In this case, the final emplacement of the Srednogorie segment could have taken place in the Latest Cretaceous or somewhat later, without vertical axis rotation.

The first event of bending could have been an about 30° of the ABT segments, in co-ordinaton with the Eastern and Western Vardar Zones (Márton et al., 2022) and the Drina-Ivanjica unit (Velki et al., 2023) of the Internal Dinarides between 20 and 17 Ma (Fig. 11). The AB segments continued the CW rotation between 17 and 15 Ma as constrained by paleomagnetic results from the Apuseni Mts (Pătrăşcu et al., 1994) due to the corner effect of Moesia combined with the continuing subduction pull of the East Carpathians.

The magnitude of the rotation of the Danubicum (combined data from the Serbian and Romanian sides of the river Danube, Table 2) which is much larger than the angle for the Timok segment, suggests that the second Miocene deformation event had an important role in orienting the Danubicum near the river Danube.

6. Conclusions

The paleomagnetic results of the present study represent two units of the East Serbian Carpathians: the Timok Magmatic Complex, belonging to the Getic unit and the Danubicum.

From the Timok Magmatic Complex, the primary magnetizations of the Upper Cretaceous igneous and sedimentary rock suggest about 25° vertical axis CW rotation. This unit represents a roughly N-S oriented segment of the Apuseni-Banat-Timok-Srednogorie (ABTS) magmatic belt of one of the largest metallogenetic province of Europe.

The popular model of post-Cretaceous oroclinal bending of an originally E-W oriented ABTS subduction zone is not plausible, since it requires about 90°CW vertical axis rotation between the Srednogorie and the Timok segments, which exceeds by about 65° the angle between the respective paleomagnetic directions. This is the main reason for the arc not being a secondary orocline, but a progressive arc, suggesting a non-linear geometry of the Cretaceous ABTS.

In our reconstruction of the main phases of bending we calculate with a E-W oriented S and a NNW-SSE oriented ABT segments in the late Cretaceous. The ABT segment changed orientation between 20 and 17 Ma due to an about 30° CW rotation, in co-ordination with the Vardar Zone. Continuing CW rotation affected the AB segments due to the corner effect of Moesia, since the CW rotations were triggered by the subduction in the Eastern Carpathians, most likely between 17 and 15 Ma.

The 69° average CW vertical axis rotation of the Danubicum fits the bending pattern between the Timok and the Banat segments, thus contributing to the paleomagnetic constrains of the circum-Moesian orocline.

CRediT authorship contribution statement

Emő Márton: Writing – original draft, Validation, Methodology, Investigation, Funding acquisition, Conceptualization. **Vesna Cvetkov:** Writing – original draft, Visualization, Methodology, Investigation, Funding acquisition. **Miodrag Banješević:** Writing – original draft, Methodology, Investigation. **Gábor Imre:** Visualization, Investigation, Formal analysis, Data curation. **Aleksandar Pačevski:** Writing – original draft, Visualization, Methodology, Investigation, Formal analysis.

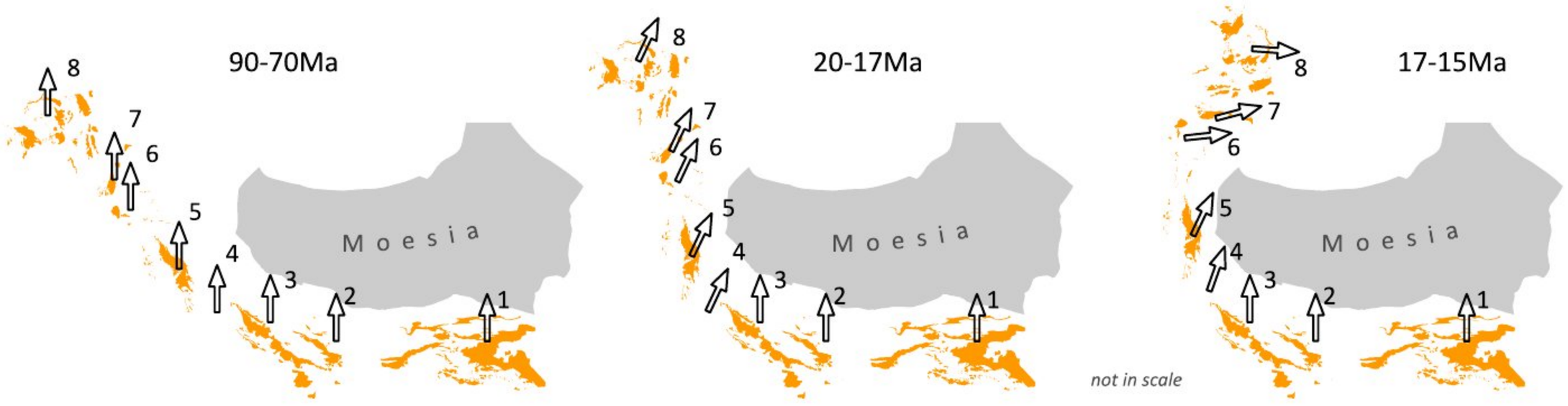

Fig. 11. Three stages of the development of the circum-Moesian orocline as suggested by the paleomagnetic declinations. Key to the simplified diagrams: orange areas are the Late Cretaceous ABTS igneous rocks and sedimentary basins (Gallhofer et al., 2015), arrows are the paleomagnetic overall-mean declinations for the respective areas with numbers referring to Fig. 9.

Declaration of Competing Interest

The authors declare the following financial interests/personal relationships which may be considered as potential competing interests Emo Marton reports financial support was provided by National Research Development and Innovation Office of Hungary. Vesna Cvetkov reports financial support was provided by Republic of Serbia Ministry of Education Science and Technological Development. Aleksandar Pačevski reports financial support was provided by Republic of Serbia Ministry of Education Science and Technological Development. If there are other authors, they declare that they have no known competing financial interests or personal relationships that could have appeared to influence the work reported in this paper.

Data availability

Data will be made available on request.

Acknowledgement

We thank Nebojša Vasić for his guidance in the Danubiucum to find suitable outcrops for paleomagnetic sampling and Vlado Milićević for covering the expenses of the sampling campaign in the Timok area and the Danubicum. We are grateful to Gábor Tari and an anonymous reviewer for suggestions to improve the manuscript. Laboratory analysis and interpretation of the data were financially supported by the National Research, Development and Innovation Office of Hungary, project K 128625. This work was also supported by funds provided by SRI based on Contract no. 451–03–65/2024–03/200126.

Appendix A. Supporting information

Supplementary data associated with this article can be found in the online version at doi:10.1016/j.jog.2024.102058.

References

Banješević, M., 2010. Upper Cretaceous magmatic suites of the Timok Magmatic Complex. Ann. Geol. De. La Penins. Balk. 71, 13–22.

Banješević, M., Cvetković, V., von Quadt, A., Ljubović Obradović, D., Vasić, N., Pačevski, A., Peytcheva, I., 2019. New constraints on the main mineralization event inferred from the latest discoveries in the bor metallogenetic zone (BMZ, East Serbia). Miner., Spec. Issue Miner. Depos. Cent. Eur. 9 (11), 672.

Banješević., M., 2021. Stratigraphy and age of rock units and mineralization in the Timok Magmatic Complex and the Bor Metallogenic Zone – a review. 52nd International October Conference on Mining and Metallurgy - IOC 2021, Proceedings, Editors: Saša Stojadinović and Dejan Petrović, November 29th – 30th, 2021, Bor, 87-92, Organizer: University Of Belgrade – Technical Faculty in Bor.

Berza, T., Draganescu, A., 1988. The Cerna-Jiu fault system (South arpathians, Romania), a major Tertiary transcurrent lineament. Dari De. seama ale Sedint. Inst. De. Geol. si Geofiz. 72-73, 43–57.

Berza, T., Iancu, V., Seghedi, A., Nicolae, I., Balintoni, I., Ciulavu, D., Bertotti, G., 1994. Exursions to South Carpathians, Apuseni Mountains and Transylvanian Basin. Field Guideb. Alcapa II, Suppl. No. 2 Rom. Jour. Tectonisc Reg. Geol. 75.

Berza, T., Constantinescu, E., Serban-Nicolae, V., 1998. Upper cretaceous magmatic series and associated mineralisation in the carpathian-balkan orogen. Resour. Geol. 48, 291–306.

Clark, A.H., Ullrich, T.D., 2004. 40Ar/39Ar age data for andesitic magmatism and hydrothermal activity in the Timok Massif, eastern Serbia: implications for metallogenetic relationships in the Bor copper-gold subprovince. Miner. Depos. 39, 256–262.

Csontos, L., Vörös, A., 2004. Mesozoic plate tectonic reconstruction of the Carpathian region. Palaeogeogr. Palaeoclimatol. Palaeoecol. 210, 1–56.

Cox, A., 1970. Latitude dependence of the angular dispersion of the geomagnetic field. Geophys. J. R. Astron. Soc. 20, 253–269.

Đoršević, M., 2004. Volcanogenic turonian and epiclastics of the senonian in the timok magmatic complex between bor and the Tupižnica Mountain, eastern Serbia. Ann. Geol. De. La Penins. Balk. 66, 63–71.

Erak, D., Matenco, L., Toljić, M., Stojadinović, U., Andriessen, P.A.M., Willingshofer, E., Ducea, M.N., 2017. From nappe stacking to extensional detachments at the contact between the Carpathians and Dinarides – the Jastrebac Mountains of Central Serbia. Tectonophysics 710-711, 162–183.

Enkin, R., 2003. The direction – correction tilt test: an all-purpose tilt/fold test for paleomagnetic studies. Earth Planet. Sci. Lett. 212, 151–166. https://doi.org/10.1016/S0012-821X(03) 00238-3.

Fisher, R., 1953. Dispersion on a Sphere. Proceedings of the Royal Society A: Mathematical (doi.org/). Phys. Eng. Sci. 217, 295–305. https://doi.org/10.1098/rspa.1953.0064.

Gallhofer, D., von Quadt, A., Peytcheva, I., Schmid, S.M., Heinrich, C.A., 2015. Tectonic, magmatic, and metallogenic evolution of the Late Cretaceous arc in the Carpathian-Balkan orogen. Tectonics 34, 1813–1836.

Gaudenyi, T., Milošević, M.V., 2023. The East Serbian carpathians: toward its definition, delineation, and relation to the south carpathians. Eur. J. Environ. Earth Sci. 4 (2), 6–10.

Hrouda, F., 1994. A technique for the measurement of thermal changes of magnetic susceptibility of weakly magnetic rocks by the CS-2 apparatus and KLY-2 Kappabridge. Geophys. J. Int. 118, 604–612.

Janković, S., 1977. The copper deposits and geotectonic setting of the tethyan eurasian metallogenetic belt. Miner. Depos. 12, 37–47.

Jelenković, R., Milovanović, D., Koželj, D., Banješević, M., 2016. The mineral resources of the bor metallogenic zone: a review (doi.org/). Geol. Croat. 69/1, 143–155. https://doi.org/10.4154/GC.2016.11.

Kirschvink, J.L., 1980. The least-squares line and plane and the analy¬sis of palaeomagnetic data (doi.org/). Geophys. J. R. Astron. Soc. 62, 699–718. https://doi.org/10.1111/j.1365-246X.1980.tb02601.

Knaak, M., Marton, I., Tosdal, R.M., Van der Toorn, J., Davidović, D., Strmbanović, I., Zdravković, M., Živanović, J., Hasson, S., 2016. Geologic setting and tectonic evolution of porphyry Cu-Au, polymetallic replacement, and sedimentary rock-hosted Au deposits in the Northwestern area of the timok magmatic complex, Serbia. Soc. Econ. Geol., Spec. Publ. 19, 1–28.

Kolb, M., von Quadt, A., Peytcheva, I., Heinrich, C.A., Fowler, S.J., Cvetković, V., 2013. Adakite-like and normal arc magmas: distinct fractionation paths in the East Serbian segment of the Balkan Carpathian Arc. J. Petrol. 54, 421–451.

Kräutner, H.G., Krstić, B., 2002. Alpine and pre-alpine structural units within Southern Carpathians and the Eastern Balkanides. Proc. XVII Congr. Carpathian–Balk. Geol. Assoc., Geol. Carpath. 53.

Kräutner, H.G., Krstić, B., 2003. Geological Map of the Carpatho–Balkanides between Mehadia, Oravița, Niš and Sofia. Geoinstitute, Belgrade.

Krstekanić, N., Matenco, L., Toljić, M., Mandić, O., Stojadinović, U., Willingshofer, E., 2020. Understanding partitioning of deformation in highly arcuate orogenic systems: inferences from the evolution of the Serbian Carpathians. Glob. Planet. Chang. 195, 103361.

Kruczyk, J., Kądziałko-Hofmokl, M., Nozharov, P., Petkov, N., Nachev, I., 1990. Palaeomagnetic studies on sedimentary Jurassic rocks from Southern Bulgaria. Phys. Earth Planet. Int. 62, 82–96.

Lips, A., Herrington, R., Stein, G., Koželj, D., Popov, K., Wijbrans, J., 2004. Refined timing of porphyry copper formation in the Serbian and Bulgarian portions of the Cretaceous Carpatho–Balkan Belt. Econ. Geol. 99, 601–609.

Lowrie, W., 1990. Identification of ferromagnetic minerals in a rock by coercivity and unblocking temperature properties. Geophys. Res. Lett. 17, 159–162. https://doi.org/10.1029/GL017i002p00159.

Luković, A., Zavašnik, J., Cvetković, V., Šarić, K., Banješević, M., Lazarov, M., Pačevski, A., 2021. Texture and composition of ferrian ilmenite from hornblende andesites of the Timok Magmatic Complex, Serbia. Neues Jahrb. F. üR. Mineral. -Abh. 65–83.

Ljubović-Obradović, D., Carevac, I., Mirković, M., Protić, N., 2011. Upper Cretaceous volcanoclastic-sedimentary formations in the Timok Eruptive Area (eastern Serbia): new biostratigraphic data from planktonic foraminifera. Geol. Carphatica 62 (5), 435–446.

Márton, E., Toljić, V., Cvetkov, V., 2022. Late and post-collisional tectonic evolution of the Adria-Europe suture in the Vardar Zone. J. Geodyn. 149, 101880 https://doi.org/10.1016/j.jog.2021.101880.

Matenco, L., 2017. Tectonics and exhumation of Romanian Carpathians: inferences from kinematic and thermochronological studies. In: Rădoane, M., Vespremeanu-Stroe, A. (Eds.), Landform Dynamics and Evolution in Romania, Springer geography. Springer, pp. 15–56.

Matenco, L., Radivojević, D., 2012. On the formation and evolution of the Pannonian Basin: constraints derived from the structure of the junction area between the Carpathians and Dinarides. Tectonics 31, TC6007.

McFadden, P.L., McElhinney, M.W., 1988. The combined analysis of remagnetization circles and direct observations in paleomagnetism. Earth Planet. Sci. Lett. 87, 161–172.

McFadden, P.L., McElhinney, M.W., 1990. Classification of the reversal test in palaeomagnetism. Geophys. J. Int. 103, 725–729.

Nagata, T., 1961. Rock magnetism. Maruyen. Tokyo (2nd edn.).

Neubauer, F., 2015. Cretaceous tectonics in Eastern Alps, Carpathians and Dinarides: two-step microplate collision and Andean-type magmatic arc associated with orogenic collapse. Rend. Online Soc. Geol. It. 37, 40–43.

Nozharov, P., Veljović, D., 1974. Paleomagnetism of some Upper Cretaceous vulcanites in the Timok eruptive region and Srednogorie. C. R. Acad. Bulg. Sci. 27, 199–200.

Nozharov, P., Veljović, D., Petkov, N.I., 1977. Results of paleomagnetic studied of some magmatic rocks in Srednogorie and Strandja. C. R. Acad. Bulg. Sci. 30, 531–533.

Nozharov, P., Petkov, N., 1984. In: Stranja-Sakhar, Symposium, Turnovo, M. (Eds.), Paleomagn. Correl. Up. Cretac. Magmat. rocks East. Sredn. Stran.-. Vol II (Part 1), 141–149.

Panaiotu, C.G., 1998. Paleomagnetic constrains on the geodynamic history of Romania. In: Ioane, D. (Ed.), Monogr. South. Carnaptians. Rep. Geod. 7/37, 205–216.

Panaiotu, C.G., Panaiotu, C.E., Lazar, I., 2012. Remagnetization of Upper Jurassic limestones from the Danubian Unit (Southern Carpatians, Romania): tectonic implications. Geol. Carpath. 63/6, 453–461.

Parma, J., Hrouda, F., Pokorný, J., Wohlgemuth, J., Suza, P., Šilinger, P., Zapletal, K., 1993. A technique for measuring temperature dependent susceptibility of weakly magnetic rocks. In: EOS, Transactions of the American Geophysical Union, 1993. Springer meeting, p. 113.

Pastor-Galán, D., Gutiérrez-Alonso, G., Weil, A.B., 2011. Oroclinal timing through joint analysis: Insights from the Ibero-Armorican Arc. Tectonophysics 507, 31–46.

Pătrăşcu, S., Bleahu, M., Panaiotu, C., 1990. Tectonic implications of paleomagnetic research into Upper Cretaceous magmatic rocks in the Apuseni Mountains, Romania. Tectonophysics 180, 309–322.

Pătrăşcu, S., Bleahu, M., Panaiotu, C., Panaiotu, C.E., 1992. The paleomagnetism of the Upper Cretaceous magmatic rocks in the Banat area of South Carpathians: tectonic implications. Tectonophysics 213, 341–352.

Pătrăşcu, S., Panaiotu, C., Seclaman, M., Panaiotu, B., 1994. Timing of rotational motion of Apuseni Mountains (Romania): Paleomagnetic data from Tertiary magmatic rocks. Tectonophysics 233, 163–176.

Prèvot, M., Hoffmann, K.A., Goguitchaichvili, a, Doikhan, J.C., Shcherbakov, V., Bina, M., 2001. The machanism of self-reversal of thermoremanence in natural hemoilmenite crystals: new experimental data and model. Phys. Earth Planet. Inter. 126, 75–92.

Ratschbacher, L., Linzer, H.G., Moser, F., Strusievicz, R.O., Bedelean, H., Har, N., Mogos, P.A., 1993. Cretaceous to Miocene thrusting and wrenching along the central South Carpathians due to a corner effect during collision and orocline formation. Tectonics 12, 855–873.

Rundić, Lj, Vasić, N., Banješević, M., Prelević, D., Gajić, V., Kostić, B., Stefanović, J., 2019. Facies analyses, biostratigraphy and radiometric dating of the Lower–Middle Miocene succession near Zaječar (Dacian basin, eastern Serbia). Ann. Géologiques De. la Péninsule Balk. 80/2, 13–37.

Schmid, S.M., Fügenschuh, B., Kounov, A., Matenco, L., Nievergelt, P., Oberhänsli, R., Pleuger, J., Schefer, S., Schuster, R., Tomljenović, B., Ustaszewski, K., van Hinsbergen, D., 2020. Tectonic units of the Alpine collision zone between Eastern Alps and western Turkey. Gondwana Res. 78, 308–374. https://doi.org/10.1016/j.gr.2019.07.005.

Thébault, E., Finlay, C.C., Beggan, C.D., Alken, P., Aubert, J., Barrois, O., Bertrand, F., Bondar, T., Boness, A., Brocco, L., Canet, E., Chambodut, A., Chulliat, A., Coïsson, P., Civet, F., Du, A., Fournier, A., Fratter, I., Gillet, N., Hamilton, B., Hamoudi, M., Hulot, G., Jager, T., Korte, M., Kuang, W., Lalanne, X., Langlais, B., Léger, J.-M., Lesur, V., Lowes, F.J., Macmillan, S., Mandea, M., Manoj, C., Maus, S., Olsen, N., Petrov, V., Ridley, V., Rother, M., Sabaka, T.J., Saturnino1, D., Schachtschneider, R., Siro, O., Tangborn, A., Thomson, A., Tøffner-Clausen, L., Vigneron, P., Wardinski, I., Zvereva, T., 2015. International Geomagnetic Reference Field: the 12th generation. Earth, Planets Space 67, 79 (article no).

Vasić, N., Obradović, J., Grubin, N., 1997. Characteristics of Jurassic system in the Danubicum Pesaca greben and Miroc area. In: Grubic, A., Berza, T. (Eds.), Geol. Djerdap Area Int. Symp. . Geol. Danub. Gorges 29–37.

Vasić, N., Rabrenović, D., Jankičević, J., 1998. Mesozoic Formations of the Eastern Serbian Danubicum. Proc. 13th Congr. Geol. Yugosl., Herceg. Novi 2, 133–144.

van Hinsbergen, D.J.J., Dupont-Nivet, G., Nakov, R., Oud, K., Panaiotu, C., 2008. No significant post-Eocene rotation of the Moesian Platform and Rhodope (Bulgaria): implications for the kinematic evolution of the Carpathian and Aegean arcs. Earth Planet. Sci. Lett. 273, 345–358.

Velki, M., Márton, E., Cvetkov, V., Kövér, S., 2023. Paleomagnetic contribution to resolving the tectonic evolution of the Drina–Ivanjica Unit, Internal Dinarides. Geol. Carpath. 74/5, 423–440.

Velojić, M., Klimentyeva, D., von Quadt, A., Guillong, M., Melcher, F., Meisel, T., Prelević, D., 2023. New insights on the geochemical affinity and age of mineralized rocks in Timok magmatic complex, East Serbia. Ann. Géologiques De. la Péninsule Balk. 84/1, 47–63.

von Quadt, A., Peytcheva, I., Cvetković, V., Banješević, M., Koželj, D., 2002. Geochronology, geochemistry and isotope tracing of the Cretaceous magmatism of East-Serbia as part of the Apuseni-Timok-Srednogorie metallogenic belt. Geol. Carpath. 53, 175–177.

von Quadt, A., Moritz, R., Peytcheva, I., Heinrich, C., 2005. Geochronology and geodynamics of Late Cretaceous magmatism and Cu-Au mineralization in the Panagyurishte region of the Apuseni-Banat-Timok-Srednogorie belt, Bulgaria. Ore Geol. Rev. 27, 95–126.

Watson, G.S., Enkin, R.J., 1993. The fold test in paleomagnetism as a parameter estimation problem. Geophys. Res. Lett. 20, 2135–2137. https://doi.org/10.1029/93GL01901.

Zijderveld, J.D.A., 1967. AC Demagnetization of Rocks: Analysis of Results. In: Runcorn, S.K., Creer, K.M., Collinson, D.W. (Eds.), Methods in Palaeomagnetism. Elsevier, Amsterdam, pp. 254–286.

Zimmerman, A., Stein, H., Hannah, J., Koželj, D., Bogdanov, K., Berza, T., 2008. Tectonic configuration of the Apuseni-Banat-Timok-Srednogorie Belt, Balkans-South Carpathians, constrained by high precision Re-Os molybdenite ages. Miner. Depos. 43, 1–21.